TÜBİTAK

Turkish Journal of Medical Sciences

http://journals.tubitak.gov.tr/medical/

Research Article

Turk J Med Sci
(2015) 45: 686-693

doi:10.3906/sag-1403-113

Efficacy of diffusion-weighted magnetic resonance imaging in the evaluation of extrahepatic cholestasis-related hepatic fibrosis

Süleyman AYVAZ[1], Sedat Alpaslan TUNCEL[2], Güray CAN[3], Bekir ÇAĞLI[2], Turan KARACA[4,*], Selim DEMİRTAŞ[4], Muhammed ELMAOĞLU[5], Mehmet Ercüment ÜNLÜ[2], Mehmet PUL[1]

[1]Department of Pediatric Surgery, Faculty of Medicine, Trakya University, Edirne, Turkey
[2]Department of Radiology, Faculty of Medicine, Trakya University, Edirne, Turkey
[3]Department of Gastroenterology, Faculty of Medicine, Trakya University, Edirne, Turkey
[4]Department of Histology and Embryology, Faculty of Medicine, Trakya University, Edirne, Turkey
[5]Medical Imaging Academy, İstanbul, Turkey

Received: 25.03.2014 • **Accepted/Published Online:** 15.10.2014 • **Printed:** 30.06.2015

Background/aim: To investigate the efficacy of diffusion-weighted magnetic resonance imaging (DWI) in the diagnosis and staging of fibrosis induced by experimental bile duct ligation (BDL).

Materials and methods: Twenty-four rats were divided randomly into four groups: control, BDL - 3 days, BDL - 2 weeks, and BDL - 4 weeks. DWI was performed with b-values of 100 and 500 on the rats from control group at day zero, on the rats from the BDL - 3 days group at the end of day 3, on the rats from the BDL - 2 weeks group at the end of day 14, and on the rats from the BDL - 4 weeks at the end of day 28.

Results: When fibrosis scores generated in all groups were evaluated together, a strong negative correlation was detected between fibrosis scores and apparent diffusion coefficient (ADC) values measured using b 100 and b 500. ADC values obtained using b 100 were found to be significantly higher compared to the fibrosis observed in both the BDL - 2 weeks and BDL - 4 weeks groups ($P < 0.003$ and $P < 0.001$, respectively).

Conclusion: We think that DWI may be an alternative to liver biopsy for the diagnosis and staging of hepatic fibrosis with underlying extrahepatic cholestasis.

Key words: Bile duct ligation, hepatic fibrosis, diffusion-weighted magnetic resonance, experimental extrahepatic cholestasis, rat

1. Introduction

Extrahepatic cholestasis is defined as a blockage of the passage of bile to the duodenum due to narrowing or lesions at the level of the common hepatic duct. The main reasons leading to extrahepatic cholestasis include common bile duct (CBD) stones, cholangiocarcinoma, ampullary carcinoma, pancreatic diseases (pancreatic head carcinoma, pseudotumoral chronic pancreatitis, pancreatic head pseudocysts), CBD strictures and congenital malformations (cysts, Caroli disease), duodenal diverticula, ascaridiasis, and hemobilia (1). In the case of bile duct obstruction, increased biliary pressure (30–40 cmH_2O) and biliary stasis cause histological changes in the liver. In acute bile duct obstruction, canalicular cholestasis and the proliferation of the bile duct cells lead to portal tract alterations. During the chronic stage, increased periductal connective tissue and fibrosis are observed (2).

Early diagnosis of the hepatic fibrosis may facilitate interventions to prevent the progression of the fibrosis to cirrhosis (3–5). Liver biopsy is still considered the gold standard for the evaluating fibrosis (6). However, this invasive method may lead to several conditions ranging from minor complications that do not require hospitalization, such as pain and bleeding, to major complications including death. Additionally, another consideration that limits liver biopsy is sampling error. As fibrosis has a heterogeneous distribution and only a small sample should be removed from the liver tissue, sampling errors are unavoidable (7,8). Due to these limitations of liver biopsy, serological tests such as the FibroTest and noninvasive methods such as elastosonography, perfusion-weighted magnetic resonance, and magnetic resonance elastography were developed to diagnose fibrosis (9).

* Correspondence: turankaraca@trakya.edu.tr

Diffusion-weighted magnetic resonance imaging (DWI) is an imaging technique that uses the diffusion properties of water molecules to illustrate tissue contrast. DWI is a technique that is commonly used in neuroradiology in order to detect intracranial infections, to characterize brain tumors, and to diagnose ischemia observed in the cerebrovascular pathologies in an early stage (10–12). The use of DWI in the differentiation and detection of malignant and benign lesions in other areas of the body and in the evaluation of pre- and posttreatment response in liver tumors is relatively new but quite promising (13). In addition, DWI was suggested to be likely to be useful in the diagnosis of hepatic fibrosis. DWI numerically measures the diffusion of water molecules in the biological tissues using an apparent diffusion coefficient (ADC). The ADC that was measured using DWI was used to characterize diffuse liver diseases, such as focal hepatic lesions and hepatic fibrosis (14).

Several studies suggested that the molecular diffusion of the water could be limited in the presence of collagen fibrils with lobular structure, which have been damaged due to hepatic fibrosis (15–17). In addition, these studies demonstrated that ADC values were decreased in fibrotic and cirrhotic hepatic tissue compared to normal liver tissue (15–17).

There are many studies showing that DWI was efficient in the evaluation of the pathologies causing fibrosis along with benign and malignant lesions of the liver (12,15–17). These studies encouraged us with the thought that this imaging technique could be useful in the diagnosis of liver injuries with underlying experimental extrahepatic cholestasis and in the follow-up of the continuing pathological course. We planned this study based on the hypothesis that, in liver injuries due to extrahepatic cholestasis, there might be a correlation between DWI findings and histopathological findings.

2. Materials and methods

2.1. Animals and experimental protocol

Male Sprague Dawley rats, weighing 180–250 g, were housed in the Experimental Animals Research Laboratory under standard laboratory conditions (22 ± 1 °C, 12-h light/dark cycle). All the experimental procedures described in this study were performed in accordance with the guidelines of the local ethics committee for animal studies. Rats were fed with standard rat feed and tap water ad libitum. All surgical procedures were performed in the Experimental Animals Research Laboratory.

Twenty-four rats were randomized into four groups (n = 6), which were designed as follows: control group; bile duct ligation (BDL) - 3 days group to form mild fibrosis; BDL - 2 weeks group to form moderate fibrosis; and BDL - 4 weeks group to form severe fibrosis. The subjects were anesthetized with 50 mg/kg intramuscular ketamine hydrochloride and 15 mg/kg intramuscular xylazine. Laparotomy was performed using a midline incision. The CBD was found between liver lobes and the duodenum and it was revealed by doing thin dissections. An extrahepatic cholestasis model was formed by cutting the CBD between the knots tied twice from the proximal of the CBD and once from its distal part using 4/0 silk sutures. The abdominal wall and skin were closed with continuous sutures using 3/0 silk suture as separate layers. At the end of the procedure, groups were placed in different cages. Hence, in the rats, pathological changes that could progress up to fibrosis were induced by forming a choledochus ligation. DWI was performed by repeating the anesthesia at day 0 in the rats of the control group, at the end of day 3 in the rats of the BDL - 3 days group, at the end of day 14 in the rats of the BDL - 2 weeks group, and at the end of day 28 in the rats of the BDL - 4 weeks group. In each group, immediately after the completion of the radiological imaging, the abdominal cavity was opened and liver tissues were removed for histopathological examination. Liver tissue samples were placed into Bouin solution.

2.2. DWI technique

All magnetic resonance imaging was performed at 63.64 MHz (1.5 Tesla Signa HDxt, General Electric, USA). The system was equipped with 33 mT/m gradient power with a slew rate of 120. A standard body coil was used as the radiofrequency transmitter and an eight-channel standard neurovascular head/neck coil was used as the receiver. An eight-channel coil was used for application of parallel imaging technique (ASSET) in order to reduce susceptibility artifacts. Standard protocol involved a three-plane localizer followed by a coil sensitivity map and a T2-weighted axial modified fast spin echo pulse sequence with repetition time (TR)/echo time (TE), 1840/68 ms; echo train length (ETL), 16; number of signal averages (NSA), 4; field of view (FOV), 180 × 144 mm^2; and matrixes, 192 × 160 with 4 mm slice thickness, which yielded 0.9 × 0.9 × 4.0 pixel size. The DWI sequence used was a modified spin-echo echo-planar imaging based pulse sequence with a b-value of 0–100 and 0–500 s/mm^2 in two separate acquisitions but with identical imaging parameters. Each b-value was acquired with b 0 in order to produce ADC maps. The diffusion gradients were applied in all three orthogonal directions. Additional DWI parameters were: TR/TE, 2000/min; FOV, 180 × 90 mm; matrixes, 64 × 48 with 4 mm slice thickness; and NSA, 8. A parallel imaging option ASSET with an acceleration factor of two was used. Measurements were done with the Functool Performance (volume share 2 - AW4.4) commercial program provided by General Electric Company on their Advantage Workstation 4.6. Initially, T2-weighted and diffusion-

weighted images were placed in a row. A region of interest (ROI) was selected from proper parenchymal tissue. An ROI area of 15 mm^2 was used for all measurements. All measurements were done on two consecutive slices that displayed proper liver parenchyma to avoid partial volume effect from results. Four ADC values were determined from both left and right liver lobes. The average was considered the parenchymal mean ADC value. The same procedure was applied to b 100 (s/mm^2) and b 500 (s/mm^2)

2.3. Histopathological examination

The liver tissues were collected and immediately fixed with 10% neutral buffered formalin and embedded in paraffin. Sections (5 μm) were prepared and then stained with hematoxylin and eosin dye for photomicroscopic observations. Liver fibrosis was evaluated by a semiquantitative method to assess the degree of histological injury using the following criteria: grade 0, normal liver (F0); grade 1, few collagen fibrils extended from the central vein to the portal tract (F1); grade 2, apparent collagen fibril extension without encompassing the whole lobule (F2); grade 3, collagen fibrils extended into and encompassing the whole lobule (F3); grade 4, diffuse extension of collagen fibrils and formation of pseudolobule (F4) (18).

2.4. Statistical analysis

All statistical analyses were completed using SPSS 15.0 for Windows. Statistical analysis of the control and the three experimental groups was compared using one-way analysis of variance (ANOVA) and the least significant difference (LSD) post hoc test. $P < 0.05$ was considered statistically significant. All values were expressed as mean ± standard deviation. Spearman's rank correlation test was used to assess the correlation between hepatic ADC and stage of fibrosis. The diagnostic performance of DWI was assessed with a receiver operating characteristic (ROC) curve. An ROC curve is a plot of sensitivity versus (1 – specificity) for all possible cutoff values. The most commonly used index of accuracy is the area under the ROC curve (AUC), with values close to 1.0 indicating high diagnostic accuracy.

3. Results

In our study, when fibrosis scores generated in all groups were evaluated together, a strong negative correlation was detected between fibrosis scores and ADC values measured using b 100 (s/mm^2) (Spearman rho = –0.747 and $P < 0.01$). Similarly, when fibrosis scores generated in all groups were evaluated together, a marked negative correlation was detected between fibrosis scores and ADC values measured using b 500 (s/mm^2) (Spearman rho = –0.743 and $P < 0.01$).

3.1. DWI findings

DWIs performed at b 100 (s/mm^2) and b 500 (s/mm^2) are shown in Figures 1a–1d and 2a–2d. In Figures 1a and 2a, images of the normal hepatic parenchymal structure obtained in the control group are shown. In the BDL - 3 days group, both b levels led to mild dilation in the bile ducts (Figures 1b and 2b). In BDL - 2 weeks (Figures 1c and 2c) and in BDL - 4 weeks (Figures 1d and 2d), both b levels led to marked dilation in the bile ducts.

While the lowest ADC values calculated using both b 100 (s/mm^2) and b 500 (s/mm^2) were obtained in the BDL - 4 weeks group, the highest ADC value was detected in the control group and it was significantly higher compared to the other groups ($P < 0.001$). At b 100 (s/mm^2), the ADC value calculated in the BDL - 3 days group was substantially higher than in the BDL - 2 weeks and BDL - 4 weeks groups, respectively ($P < 0.003$ and $P < 0.001$). However, ADC values were not significantly different between the BDL - 2 weeks and BDL - 4 weeks groups ($P > 0.05$). When b 500 (s/mm^2) was used, the ADC value calculated in the BDL - 3 days group was significantly higher than in the BDL - 4 weeks group ($P < 0.002$), whereas it was not significantly different in the BDL - 2 weeks group ($P > 0.05$). On the other hand, when b 500 (s/mm^2) was used, the ADC value measured in the BDL - 2 weeks group was substantially higher compared to the BDL - 4 weeks group ($P < 0.02$). ADC values calculated using b 100 (s/mm^2) and b 500 (s/mm^2) for the groups are given in the Table.

3.2. Histopathological findings

Histopathological examination of the control liver showed normal liver tissue. The control rats showed no fibrosis (Figure 3a). In the BDL - 3 days group, inflammatory cell infiltration and fibrosis had begun (Figure 3b). In the BDL - 2 weeks group, ductular proliferation was added to the fibrotic process (Figure 3c). In the BDL - 4 weeks group, dense inflammatory cell infiltration, ductular proliferation, and diffuse fibrosis were noteworthy (Figure 3d).

While fibrosis score was significantly higher in the BDL - 3 days group than in the control group ($P < 0.001$), it was substantially lower in the BDL - 3 days group compared to the BDL - 2 weeks group ($P < 0.001$). While the fibrosis score was markedly higher in the BDL - 2 weeks group compared to the control group ($P < 0.0001$), it was substantially lower compared to the BDL - 4 weeks group ($P < 0.001$). The fibrosis score obtained in the BDL - 4 weeks group was markedly higher than in the control and BDL - 3 days groups ($P < 0.0001$). The results of the fibrosis scores for each group are given in the Table.

3.3. Assessment of fibrosis by DWI and fibrosis scores

ROC curves were used to analyze the usefulness of ADC values for predicting fibrosis stage. For the differentiation of the absence of fibrosis and mild fibrosis (F0–F1) from moderate and severe fibrosis (F2–F4), ADC values obtained using b 100 (s/mm^2) had an AUC of 0.868, sensitivity of 80.00%, and specificity of 92.86%. For the differentiation of the absence of fibrosis and mild fibrosis

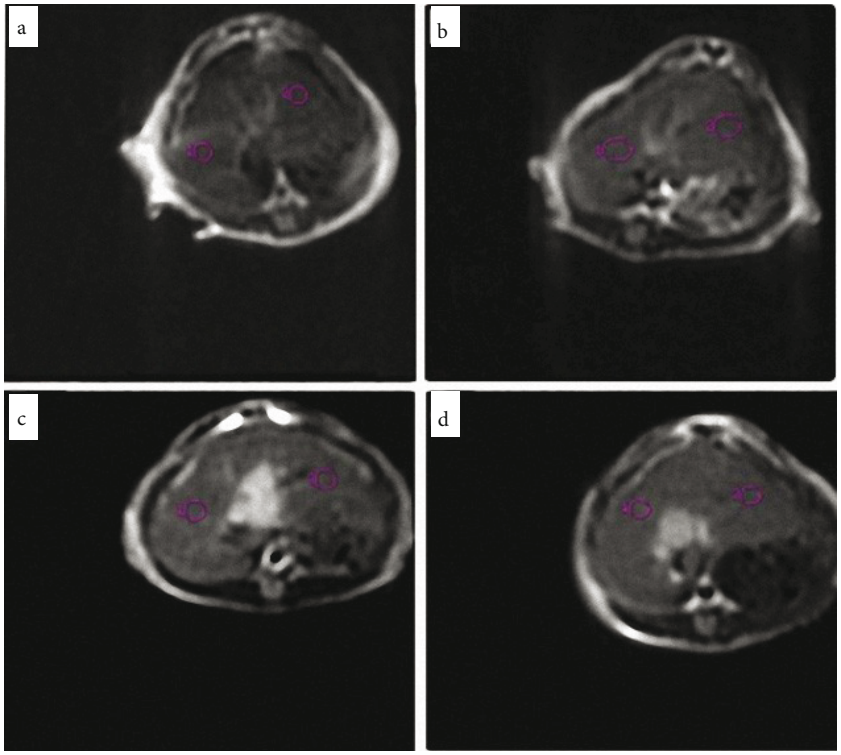

Figure 1. DWI (b 100) of the liver: a) Control group. b) Mild dilatation of the central bile ducts is seen in BDL - 3 days group. c) Significant dilatation of central bile ducts is seen in BDL - 2 weeks group. d) BDL - 4 weeks group.

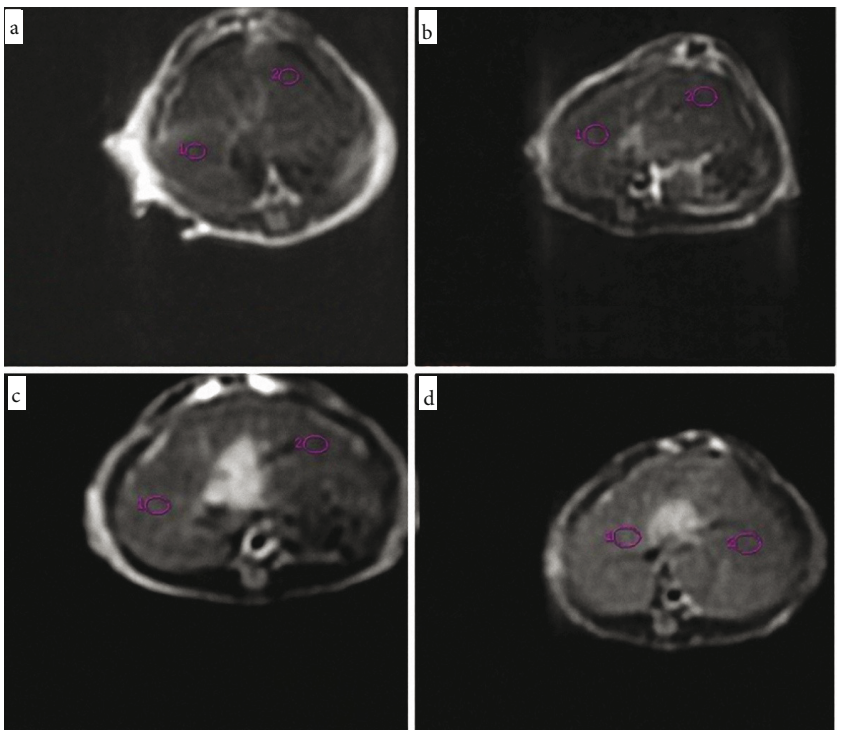

Figure 2. DWI (b 500) of the liver; ADC values are lower than those for b 100 (see Table): a) Control group. b) BDL - 3 days group. c) BDL - 2 weeks group. d) BDL - 4 weeks group.

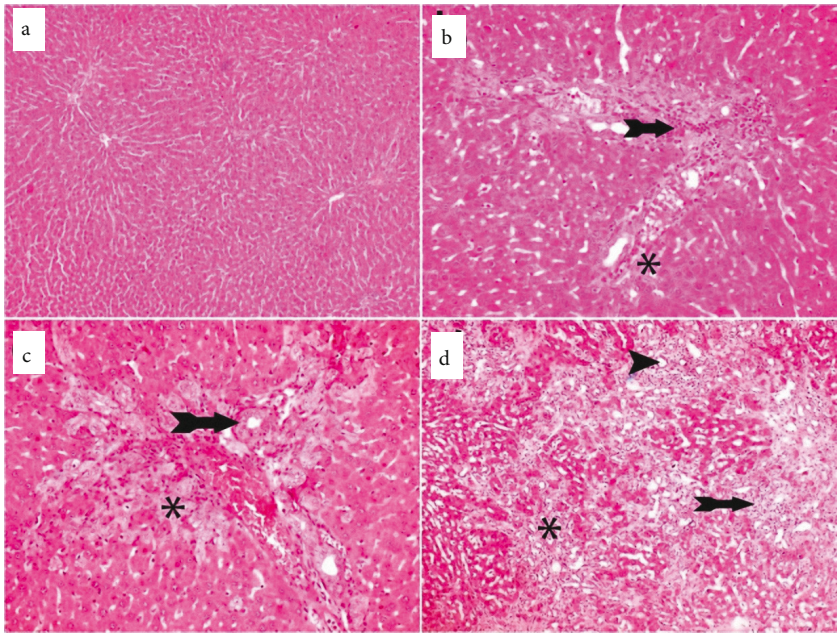

Figure 3. a) Control group, normal liver tissue. b) From 3 days after BDL, inflammatory cell infiltration (arrow) and fibrosis (*) were predominant. c) From 2 weeks after BDL, ductular proliferation (arrow) and fibrosis (*). d) From 4 weeks after BDL, intensive inflammatory cell infiltration (arrow), ductular proliferation (arrowhead), and diffuse fibrosis (*). H&E, magnification: a and d, 100×; b and c, 200×.

Table. The apparent diffusion coefficients (ADCs) and fibrosis scores for each group.

	Control	BDL - 3 days	BDL - 2 weeks	BDL - 4 weeks
ADC ($\times 10^{-3}$ mm^2/s) (using b 100 s/mm^2)	5.07 ± 0.60[a]	3.17 ± 0.65[b,c]	2.16 ± 0.49	2.04 ± 0.24
ADC ($\times 10^{-3}$ mm^2/s) (using b 500 s/mm^2)	2.25 ± 0.24[a]	1.70 ± 0.26[d]	1.56 ± 0.10[e]	1.26 ± 0.18
Fibrosis score	0.00 ± 0.00	1.67 ± 0.81[f]	2.33 ± 0.81[g,c]	3.00 ± 0.63[h]

Values are expressed as mean ± SD; n = 6 for each group.

[a] $P < 0.0001$ compared with BDL - 3 days, BDL - 2 weeks, and BDL - 4 weeks.

[b] $P < 0.003$ compared with BDL - 2 weeks.

[c] $P < 0.001$ compared with BDL - 4 weeks.

[d] $P < 0.002$ compared with BDL - 4 weeks.

[e] $P < 0.02$ compared with BDL - 4 weeks.

[f] $P < 0.001$ compared with control and BDL - 2 weeks.

[g] $P < 0.0001$ compared to control.

[h] $P < 0.0001$ compared to control and BDL - 3 days.

(F0–F1) from moderate and severe fibrosis (F2–F4), ADC values obtained using b 500 (s/mm^2) had an AUC of 0.875, sensitivity of 80.00%, and specificity of 100.00% (Figure 4).

4. Discussion

Cholestasis may result from bile duct obstruction and accumulation of the bile in the liver due to several pathologies, such as obstructive, inflammatory, and genetic conditions. Increased pressure in the bile ducts leads to the accumulation of toxic substances and to macroscopic and microscopic changes in the liver, preventing bile flow. When obstruction persists, fibrosis and consequently biliary cirrhosis develop around the bile ducts (19).

The rat model of hepatic fibrosis induced by CBD ligation is an interesting fibrosis model used in the most recent scientific studies because it forms rapidly and complies with primary or secondary biliary cirrhosis in humans. When CBD ligation is administered to rats, it forms extracellular matrix proteins, especially collagen, in the liver, and it is a suitable model for the development of secondary hepatic fibrosis in rats (20). In our study, we used this model in order to form fibrosis in the liver.

It is difficult to evaluate hepatic fibrosis and inflammation using conventional MRI (21). Several studies demonstrated that ADC values were lower in the cirrhotic liver compared to normal livers (22–26).

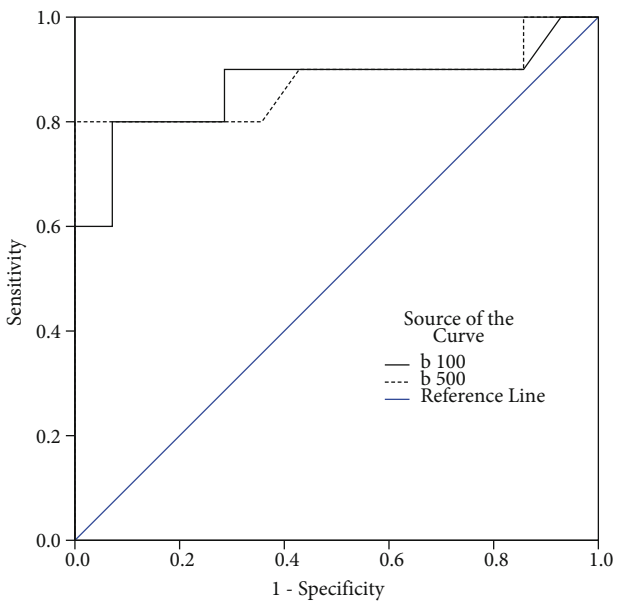

Figure 4. ROC curve with ADC for differentiating absence of fibrosis (F0) and mild fibrosis (F1) from moderate to severe fibrosis (F2–F4). For b 100 (s/mm^2) the AUC is 0.868 with a sensitivity of 80.00% and specificity of 92.86%. ADC criterion value is $\leq 2.90 \times 10^{-3}$ mm^2/s. For b 500 (s/mm^2) the AUC is 0.875 with a sensitivity of 80.00% and specificity of 100.00%. The ADC criterion value $\leq 1.82 \times 10^{-3}$ mm^2/s.

In a study performed by Koinuma et al. (15) on a large series of subjects using a low b-value (128 s/mm^2), it was demonstrated that there was an important negative correlation between ADC and fibrosis score, but there was no correlation between ADC values and the degree of inflammation. Sandrasegaran et al. (Spearman rho = –0.36) and Taouli et al. (Spearman rho = –0.45) reported a moderately negative correlation between ADC values and fibrosis stages (27,28). In our study, when evaluated along with the grades of fibrosis observed in all groups, the finding of a strong negative correlation between ADC values obtained with both b 100 (s/mm^2) and b 500 (s/mm^2) showed consistency with the results of those studies. On the other hand, Boulanger et al. could not detect a significant correlation between ADC values and fibrosis and inflammation grades (29). However, when evaluating the results obtained by Boulanger et al., it should be considered that this study was conducted with a small sample size (18 patients with hepatitis C and 10 controls), which could be a potential limiting factor for the power of the study.

In a clinical study performed by Lewin et al. (54 patients with chronic hepatitis C and 20 healthy volunteers), the efficacies of serum markers of fibrosis and sonographic elastography technique were compared using DWI (using b-values of 0, 200, 400, and 800 s/mm^2) (30). In this study, it was reported that ADC could predict moderate and severe fibrosis well. In addition, it was demonstrated that ADC values were substantially lower in patients with moderate and severe fibrosis (F2–F4) compared to patients without fibrosis or with mild fibrosis (F0–F1) and to healthy volunteers. Similarly, in our study, ADC values were significantly lower in the BDL - 2 weeks (moderate fibrosis) and BDL - 4 weeks (severe fibrosis) groups compared to the control and BDL - 3 (mild fibrosis) groups. Additionally, Lewin et al. reported that the sensitivity and specificity of the ADC values were both 87% in the differentiation of patients with F3–F4 fibrosis from those with F0–F2 fibrosis. Girometti et al. reported that ADC values had sensitivity and specificity of 92% and 100%, respectively, and were significantly lower in cirrhotic patients compared to healthy volunteers (31). In another study, it was reported that ADC values were important in the prediction of F2 or greater fibrosis and F3 or greater fibrosis, and their sensitivities were 83.3% and 88.9% and their specificities were 83.3% and 80.0%, respectively (17). Sandrasegaran et al. detected that, in the differentiation of F0–F1 fibrosis and F2–F4 fibrosis in patients with chronic viral hepatitis, ADC values had sensitivity and specificity of 72.6% and 59.3%, respectively (27). However, in our study, we detected that ADC values had higher sensitivity and specificity rates in the differentiation of the same fibrosis stages.

ADC measurement depends on many factors (32,33). Among these factors, b-level is very important for calculating ADC. ADC measurements performed using images obtained with higher b-values are more sensitive and the ADC values obtained are generally lower than the values obtained using b-values of less than 500 s/mm^2. However, compared to b-values above 800 s/mm^2, ADC values calculated using an intermediate b-value of 400 s/mm^2 may be more advantageous in the evaluation of hepatic fibrosis (31). It is known that hepatic perfusion is substantially decreased in cirrhotic patients compared to healthy people (34). Annet et al. detected a negative correlation between the decrease of ADC values and increased fibrosis scores in rats in which hepatic fibrosis was formed and they reported that, after the sacrifice of the rats, no significant difference was found between ADC values (35). As a result, it was reported that, in the evaluation of hepatic fibrosis using DWI, a decrease of liver perfusion had a greater effect on ADC values compared to the limitation of the water diffusion in the hepatic fibrosis. In another clinical study, a decrease of ADC values was demonstrated with decreasing perfusion in cirrhotic patients (16). Lower b-values are more sensitive to the effects of decreased perfusion and may be more efficient in differentiating hepatic fibrosis stages (27). In our study, the ADC values in the control group were consistent with the values of previous reports (16,35), and ADC values obtained with a low b-value (b 100 s/mm^2) were significantly higher in early-stage mild fibrosis (BDL - 3 days) than in both moderate (BDL - 2 weeks) and severe (BDL - 4 weeks) fibroses; however, ADC values were not significantly different between the BDL - 2 weeks and BDL - 4 weeks groups. On the other hand, ADC values obtained with a higher b-value (b 500 m/mm^2) in the mild fibrosis (BDL - 3 days) were only significantly different from the values for severe (BDL - 4 weeks) fibrosis. These results suggested that low b-values may be more efficient in differentiating between early fibrosis and other fibrosis stages (moderate and severe). However, while ADC values obtained with a low b-value (b 100 s/mm^2) did not show a significant difference between moderate (BDL - 2 weeks) and severe (BDL - 4 weeks) fibroses, ADC values calculated using a high b-value (b 500 s/mm^2) showed a significant difference. Our results suggest that high b-values may be more efficient in the differentiation of moderate and severe fibroses.

In conclusion, we observed a negative correlation between ADC values and the grade of the hepatic fibrosis that developed with underlying experimental BDL, in parallel with our baseline hypothesis. In addition, we found a significant difference between fibrosis scores and ADC values. In light of these results, we think that DWI may be useful in the diagnosis of several diseases that cause extrahepatic cholestasis-related hepatic fibrosis, in the staging of fibrosis, and in the evaluation of the therapeutic response. We think that, due to likely minor or major biopsy complications, the noninvasive nature of DWI makes it a viable alternative to liver biopsy. We suggest that clinical studies conducted on large series of patients who developed extrahepatic cholestasis due to several diseases would be useful.

References

1. Rogoveanu I, Gheonea DI, Saftoiu A, Ciurea T. The role of imaging methods in identifying the causes of extrahepatic cholestasis. J Gastrointestin Liver Dis 2006; 15: 265–271.
2. Slott PA, Liu MH, Tavoloni N. Origin, pattern and mechanism of bile duct proliferation following biliary obstruction in the rat. Gastroenterology 1990; 99: 466–477.
3. Wanless IR, Nakashima E, Sherman M. Regression of human cirrhosis. Morphologic features and the genesis of incomplete septal cirrhosis. Arch Pathol Lab Med 2000; 124: 1599–1607.
4. Arthur MJ. Reversibility of liver fibrosis and cirrhosis following treatment for hepatitis C. Gastroenterology 2002; 122: 1525–1528.
5. Veldhuijzen IK, Toy M, Hahné SJ, De Wit GA, Schalm SW, de Man RA, Richardus JH. Screening and early treatment of migrants for chronic hepatitis B virus infection is cost-effective. Gastroenterology 2010; 138: 522–530.
6. Berg T, Sarrazin C, Hinrichsen H, Buggisch P, Gerlach T, Zachoval R, Zeuzem S. Does noninvasive staging of fibrosis challenge liver biopsy as a gold standard in chronic hepatitis C? Hepatology 2004; 39: 1456–1467.
7. Afdhal NH, Nunes D. Evaluation of liver fibrosis: a concise review. Am J Gastroenterol 2004; 99: 1160–1174.
8. Kugelmas M. Liver biopsy. Am J Gastroenterol 2004; 99: 1416–1417.
9. Bakan AA, Inci E, Bakan S, Gokturk S, Cimilli T. Utility of diffusion-weighted imaging in the evaluation of liver fibrosis. Eur Radiol 2012; 22: 682–687.
10. Bammer R. Basic principles of diffusion-weighted imaging. Eur J Radiol 2003; 45: 169–184.
11. Naganawa S, Kawai H, Fukatsu H, Sakurai Y, Aoki I, Miura S, Mimura T, Kanazawa H, Ishigaki T. Diffusion-weighted imaging of the liver: technical challenges and prospects for the future. Magn Reson Med Sci 2005; 4: 175–186.

12. Charles-Edwards EM, de Souza NM. Diffusion-weighted magnetic resonance imaging and its application to cancer. Cancer Imaging 2006; 6: 135–143.

13. Thoeny HC, De Keyzer F. Extracranial applications of diffusion-weighted magnetic resonance imaging. Eur Radiol 2007; 17: 1385–1393.

14. Cheung JS, Fan SJ, Gao DS, Chow AM, Man K, Wu EX. Diffusion tensor imaging of liver fibrosis in an experimental model. J Magn Reson Imaging 2010; 32: 1141–1148.

15. Koinuma M, Ohashi I, Hanafusa K, Shibuya H. Apparent diffusion coefficient measurements with diffusion-weighted magnetic resonance imaging for evaluation of hepatic fibrosis. J Magn Reson Imaging 2005; 22: 80–85.

16. Luciani A, Vignaud A, Cavet M, Nhieu JT, Mallat A, Ruel L, Laurent A, Deux JF, Brugieres P, Rahmouni A. Liver cirrhosis: intravoxel incoherent motion MR imaging—pilot study. Radiology 2008; 249: 891–899.

17. Taouli B, Chouli M, Martin AJ, Qayyum A, Coakley FV, Vilgrain V. Chronic hepatitis: role of diffusion-weighted imaging and diffusion tensor imaging for the diagnosis of liver fibrosis and inflammation. J Magn Reson Imaging 2008; 28: 89–95.

18. Cemek M, Aymelek F, Büyükokuroğlu ME, Karaca T, Büyükben A, Yilmaz F. Protective potential of Royal Jelly against carbon tetrachloride induced-toxicity and changes in the serum sialic acid levels. Food Chem Toxicol 2010; 48: 2827–2832.

19. Boyer JL. New perspectives for the treatment of cholestasis: lessons from basic science applied clinically. J Hepatol 2007; 46: 365–371.

20. Montilla P, Cruz A, Padillo FJ, Tunez I, Gasson F. Melatonin versus vitamin E as protective treatment against oxidative stress after extra-hepatic bile duct ligation in rats. J Pineal Res 2001; 31: 138–144.

21. Taouli B, Koh DM. Diffusion-weighted MR imaging of the liver. Radiology 2010; 254: 47–66.

22. Taouli B, Vilgrain V, Dumont E, Daire JL, Fan B, Menu Y. Evaluation of liver diffusion isotropy and characterization of focal hepatic lesions with two single-shot echo-planar MR imaging sequences: prospective study in 66 patients. Radiology 2003; 226: 71–78.

23. Ichikawa T, Haradome H, Hachiya J, Nitatori T, Araki T. Diffusion-weighted MR imaging with a single-shot echo-planar sequence: detection and characterization of focal hepatic lesions. AJR Am J Roentgenol 1998; 170: 397–402.

24. Namimoto T, Yamashita Y, Sumi S, Tang Y, Takahashi M. Focal liver masses: characterization with diffusion-weighted echo-planar MR imaging. Radiology 1997; 204: 739–744.

25. Amano Y, Kumazaki T, Ishihara M. Single-shot diffusion-weighted echo-planar imaging of normal and cirrhotic livers using a phased-array multicoil. Acta Radiol 1998; 39: 440–442.

26. Aubé C, Racineux PX, Lebigot J, Oberti F, Croquet V, Argaud C, Calès P, Caron C. Diagnosis and quantification of hepatic fibrosis with diffusion weighted MR imaging: preliminary results. J Radiol 2004; 85: 301–306.

27. Sandrasegaran K, Akisik FM, Lin C, Tahir B, Rajan J, Saxena R, Aisen AM. Value of diffusion-weighted MRI for assessing liver fibrosis and cirrhosis. AJR Am J Roentgenol 2009; 193: 1556–1560.

28. Taouli B, Tolia AJ, Losada M, Babb JS, Chan ES, Bannan MA, Tobias H. Diffusion-weighted MRI for quantification of liver fibrosis: preliminary experience. AJR Am J Roentgenol 2007; 189: 799–806.

29. Boulanger Y, Amara M, Lepanto L, Beaudoin G, Nguyen BN, Allaire G, Poliquin M, Nicolet V. Diffusion-weighted MR imaging of the liver of hepatitis C patients. NMR Biomed 2003; 16: 132–136.

30. Lewin M, Poujol-Robert A, Boëlle PY, Wendum D, Lasnier E, Viallon M, Guéchot J, Hoeffel C, Arrivé L, Tubiana JM et al. Diffusion-weighted magnetic resonance imaging for the assessment of fibrosis in chronic hepatitis C. Hepatology 2007; 46: 658–465.

31. Girometti R, Furlan A, Esposito G, Bazzocchi M, Como G, Soldano F, Isola M, Toniutto P, Zuiani C. Relevance of b-values in evaluating liver fibrosis: a study in healthy and cirrhotic subjects using two single-shot spin-echo echo-planar diffusion-weighted sequences. J Magn Reson Imaging 2008; 28: 411–419.

32. Norris DG. The effects of microscopic tissue parameters on the diffusion weighted magnetic resonance imaging experiment. NMR Biomed 2001; 14: 77–93.

33. Le Bihan D. Molecular diffusion, tissue microdynamics and microstructure. NMR Biomed 1995; 8: 375–386.

34. Annet L, Materne R, Danse E, Jamart J, Horsmans Y, Van Beers BE. Hepatic flow parameters measured with MR imaging and Doppler US: correlations with degree of cirrhosis and portal hypertension. Radiology 2003; 229: 409–414.

35. Annet L, Peeters F, Abarca-Quinones J, Leclercq I, Moulin P, Van Beers BE. Assessment of diffusion-weighted MR imaging in liver fibrosis. J Magn Reson Imaging 2007; 25: 122–128.